IJCRT.ORG ISSN : 2320-2882

INTERNATIONAL JOURNAL OF CREATIVE RESEARCH THOUGHTS (IJCRT)

An International Open Access, Peer-reviewed, Refereed Journal

Enhanced Gas Detection in Hyperspectral Images With 3 CNN and Autoencoder Models

P.Jaya Chowdaiah[1] Mrs.K.Rupa[2]

[1]PG student, Vemu Institute of Technology, P. Kothakota.

[2]Assistant Professor,Vemu Institute of Technology, P.kothakota.

ABSTRACT

This pioneering project tackles the pressing issue of gas emission detection, crucial for environmental and human well-being. Conventional detection systems face limitations, prompting the exploration of hyperspectral image analysis for a safer and more efficient solution. Introducing a groundbreaking deep learning methodology for hyperspectral gas detection in the longwave infrared spectrum, this project merges unmixing and classification techniques. Through a specialized 3-D convolutional neural network and autoencoder-based network, it converts radiance data to luminance-temperature data, achieving remarkable performance surpassing conventional methods. Further innovation extends the approach with an Ensemble model, integrating CNN, Bi-directional, and GRU algorithms, enhancing input features for improved prediction accuracy. This innovative endeavor underscores the efficacy of modern techniques in addressing environmental challenges.

Keywords: Gas, 3D CNN

INTRODUCTION

Over the past three decades, imaging spectroscopy has been indispensable in identifying materials and their compositions, with hyperspectral remote sensing emerging in the mid-80s as a powerful tool for mineral mapping. As gas leaks become a pressing environmental concern, especially in developed countries, the need for effective monitoring solutions intensifies. Traditional methods fall short, prompting the adoption of infrared remote sensing technology for safer and more efficient gas detection. Forward-looking infrared hyperspectral cameras, operating in medium-wave and long-wave infrared bands, offer a promising approach. Previous studies have employed statistical detection methods and signal processing operations for gas detection, yet innovative approaches are needed. This project pioneers a novel deep learning-based methodology for hyperspectral gas detection, aiming to enhance environmental monitoring and mitigate risks associated with gas emissions.

LITERATURE SURVEY

A. Vallières *et al*

Standoff detection and quantification of gaseous chemicals are vital across various sectors. Meeting sensor demands necessitates high sensitivity, minimal false alarms, and real-time functionality in a portable, durable package. Thermal infrared technology has historically facilitated chemical sensing, either through spectrometers or imagers. However, recent advances in high-speed, large-format infrared imaging arrays enable unparalleled performance in spectral, spatial, and temporal domains. Integrating spatial and spectral data holds significant promise for enhancing passive detection and identification of chemical agents. This paper introduces algorithms tailored for hyperspectral imagers in the thermal infrared, demonstrating their efficacy through field data acquired with Telops FIRST imaging spectrometer.

C. C. Funk *et al*

By integrating matched filters with modified k-means clustering, this study enhances the detection of subtle signatures in hyperspectral data. Investigating various bivariate scenarios, the research elucidates the symbiotic relationship between filtering and partitioning, showcasing how clustering minimizes within-class variance and groups correlated pixels. The modified k-means algorithm, operating on image samples iteratively, exhibits improved convergence with a novel "extreme" centroid initialization method. Comparative analysis across different filtering formulations demonstrates the superiority of clutter matched filters, outperforming simple matched filters by an order of magnitude. Clustering amplifies filter efficacy by two to five times, with clutter matched filtering achieving a fifty-fold improvement, enabling the detection of faint signals in hyperspectral imagery.

S. Kumar *et al*

Efficient analysis of hyperspectral imagery is crucial for swiftly gathering actionable insights on areas affected by atmospheric gases like CH4. Current methods require manual inspection and annotation of massive datasets, posing scalability challenges and human error risks. Introducing Hyperspectral Mask-RCNN (H-mrcnn), this project integrates principled statistics, signal processing, and deep neural networks to overcome these limitations. H-mrcnn employs fast algorithms to analyze large-area hyperspectral data, autonomously detecting CH4 plumes through match-filtering sliding windows. By optimizing matched-filtering and ensemble learning, H-mrcnn achieves 85% matching accuracy with expert annotation, significantly reducing processing time and offering rapid insights into gas plumes.

PROBLME STATEMNET:

Over the past century, industrial advancements have propelled global progress, yet the resultant waste poses a grave threat to the environment. It's imperative to monitor gas emissions from industrial sectors to mitigate pollution and safeguard our natural surroundings.

PROPOSED METHOD:

This paper proposes a novel approach using a 3D-CNN autoencoder-decoder model to predict various gas emissions. Utilizing hyperspectral images captured by drones or satellites, the author applies the Spectral Angle Mapper (SAM) distance formula to discern gas leaks. SAM calculates pixel distances, matched against the NIST database, linking distance values to specific gases. This method enables the identification of gas presence in the images by correlating SAM distances, providing a valuable tool for detecting and monitoring industrial gas emissions.

ARCHITECTURE

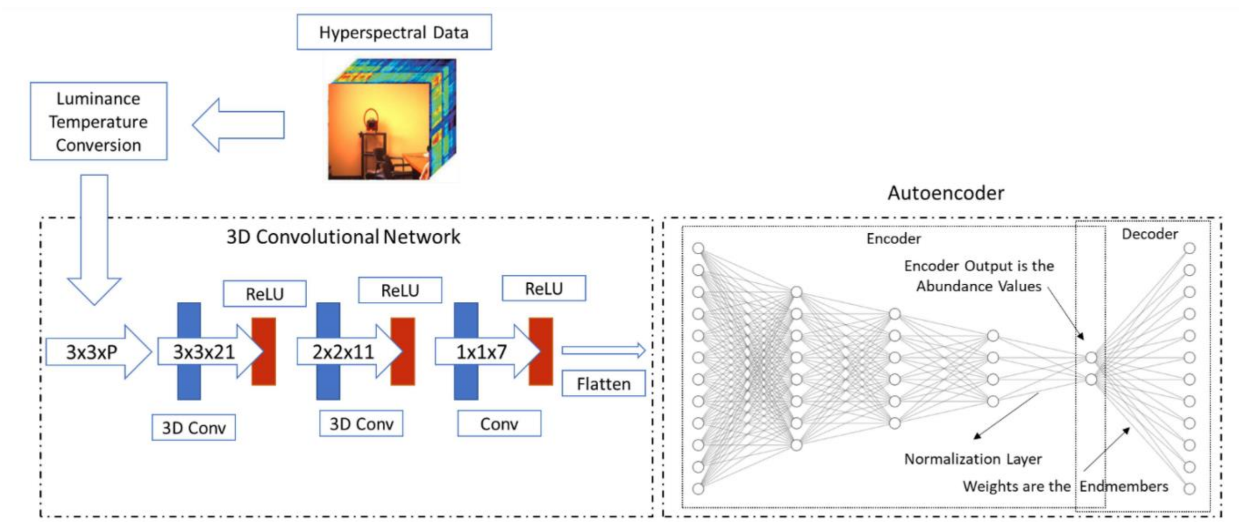

METHANE AND SULPHUR LEAK DATASET:

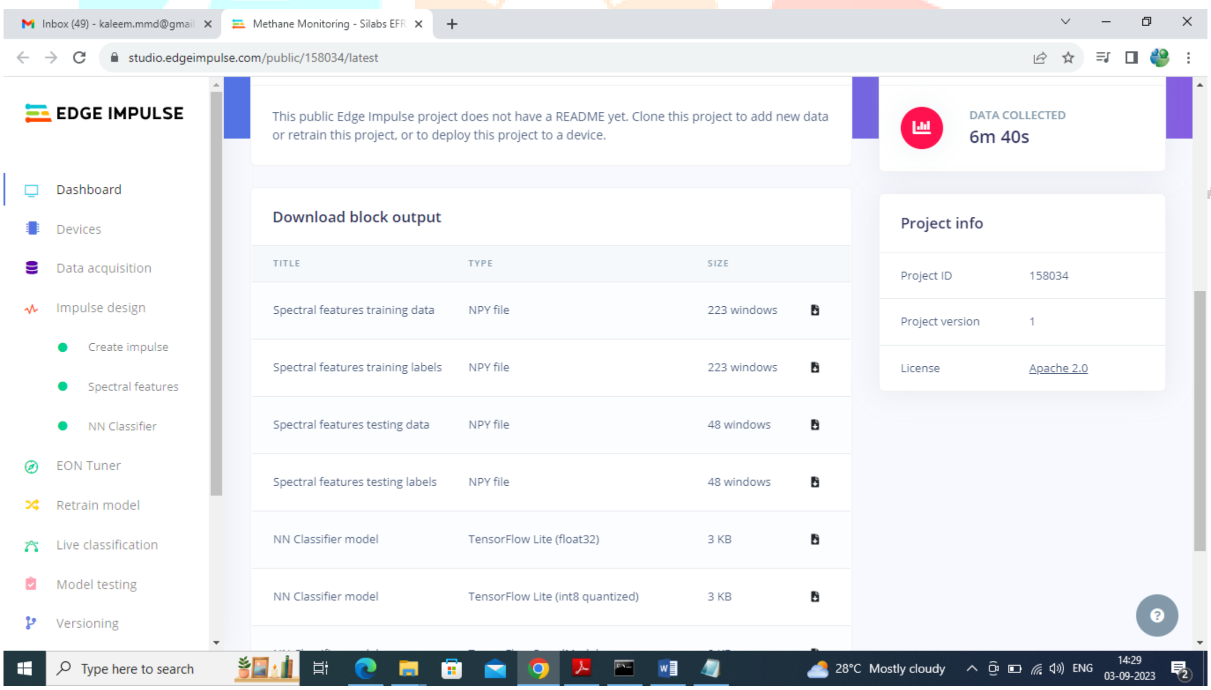

In above dataset page we have spectral features and labels for testing and by using above features we are training and test performance of propose 3D-CNN model.

METHODOLOGY:

1. Dataset Preprocessing:

Hyperspectral spectrum images are loaded from the dataset, captured by drones or satellites, containing features related to gas emissions.

The dataset labels are adjusted to represent two classes: methane and sulfur dioxide leaks.

Dataset shuffling and splitting are performed to create training and testing sets, with 80% for training and 20% for testing.

The dataset is reshaped into 4-dimensional data suitable for 3D Convolutional Neural Network (3D-CNN) training.

2. Model Training: Propose 3D-CNN Encoder-Decoder Model

A 3D-CNN model architecture is defined, comprising convolutional and pooling layers for feature extraction.

Batch normalization and dropout layers are added to prevent overfitting and enhance model generalization.

The model is compiled with the Adam optimizer and categorical cross-entropy loss function.

If the pre-trained weights are not available, the model is trained using the training dataset.

Model performance is evaluated using accuracy, precision, recall, F1-score, and confusion matrix.

3. Model Extension: CNN + Bidirectional GRU Model

An extension model is proposed by combining Convolutional Neural Network (CNN) with Bidirectional Gated Recurrent Unit (BiGRU) layers.

CNN layers extract spatial features, while BiGRU layers capture temporal dependencies in the data.

The model is compiled and trained similarly to the propose 3D-CNN model.

Performance metrics are calculated and compared with the propose model.

4. Evaluation and Analysis:

Accuracy, precision, recall, and F1-score are calculated for both models on the test dataset.

Confusion matrices are plotted to visualize model performance.

Training accuracy graphs are plotted to compare the training progress of both models over epochs.

Performance graphs are generated to illustrate the accuracy, precision, recall, and F1-score of each algorithm.

5. Deployment and Testing:

The trained models are used to predict gas emissions from test data.

Test data samples are provided, and the models predict the presence of methane or sulfur dioxide leaks.

Predictions are evaluated against actual labels to assess model accuracy and reliability.

RESULTS:

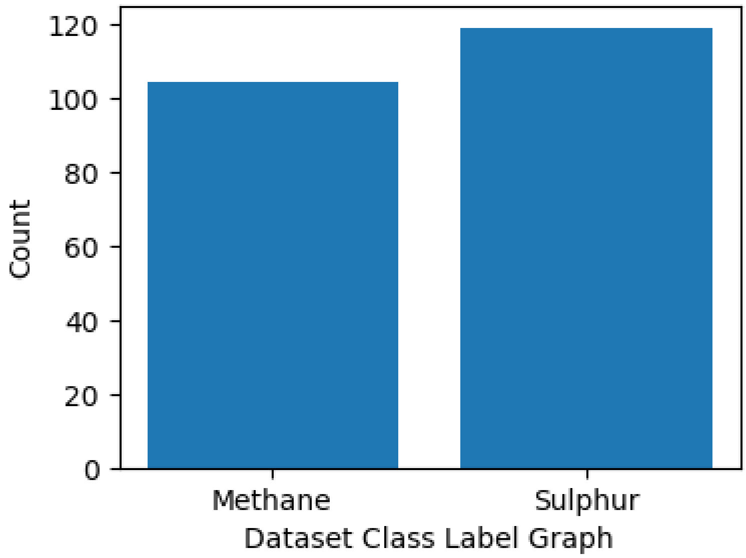

In above finding and plotting graph of different gases emission found in dataset where x-axis contains gas names and y-axis contains count of those gas leaks found in dataset

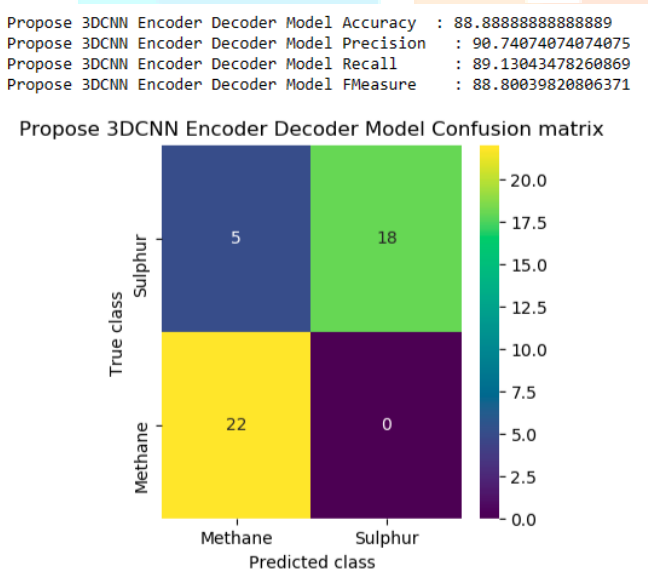

In above propose 3DCNN got 88% accuracy and can see other metrics also and in confusion matrix graph x-axis represents Predicted Labels and y-axis represents True Labels. Yellow and green boxes contains correct prediction count and blue boxes contains incorrect prediction count.

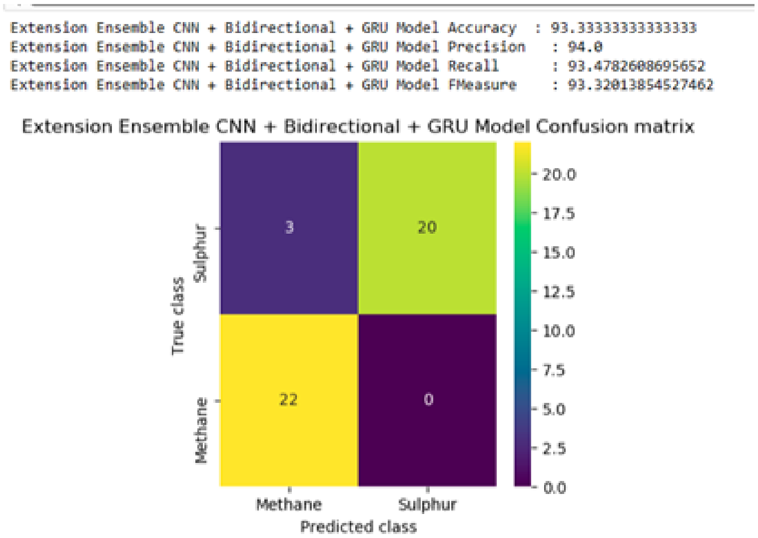

In above extension model got 93% accuracy.

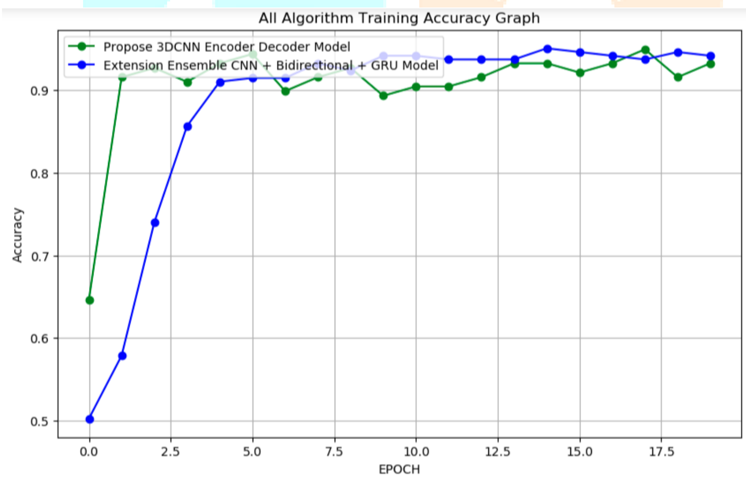

In above graph x-axis represents training epoch and y-axis represents accuracy and green line represents propose algorithm and blue line extension training accuracy where extension got high accuracy

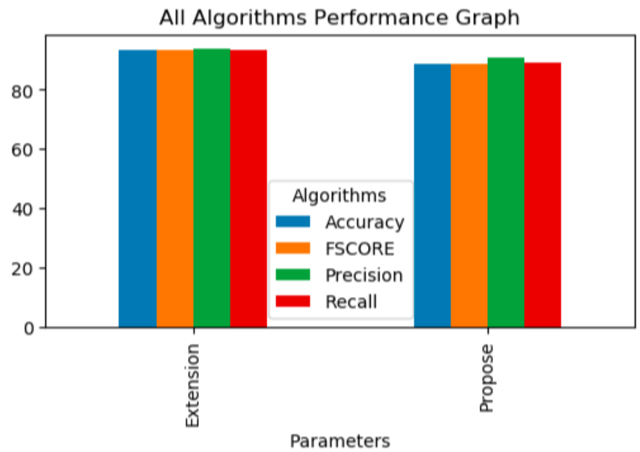

In above displaying both algorithm performance in tabular format where x-axis represents algorithm names and y-axis represents accuracy and other metrics in different colour bars

Prediction:

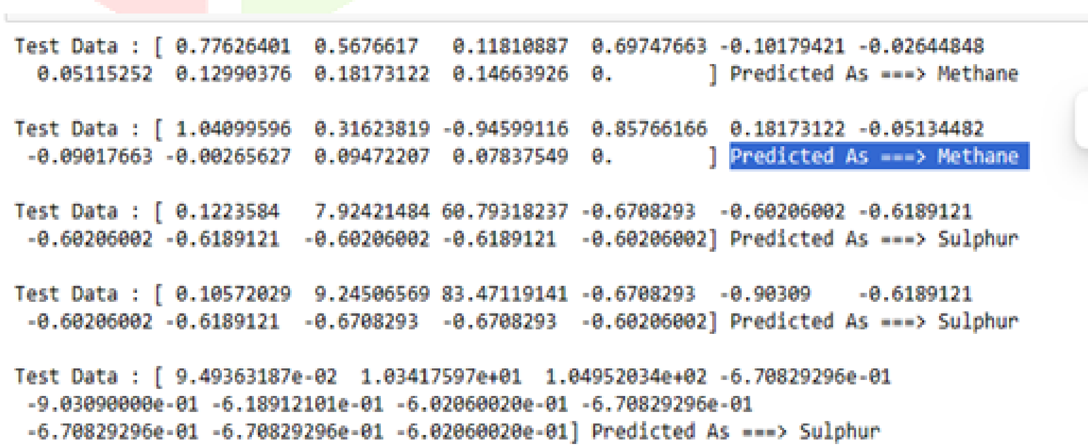

```
Test Data : [ 0.77626401  0.5676617   0.11810887  0.69747663 -0.10179421 -0.02644848
  0.05115252  0.12990376  0.18173122  0.14663926  0.         ] Predicted As ===> Methane

Test Data : [ 1.04099596  0.31623819 -0.94599116  0.85766166  0.18173122 -0.05134482
 -0.09017663 -0.00265627  0.09472207  0.07837549  0.         ] Predicted As ===> Methane

Test Data : [ 0.1223584   7.92421484 60.79318237 -0.6708293  -0.60206002 -0.6189121
 -0.60206002 -0.6189121  -0.60206002 -0.6189121  -0.60206002] Predicted As ===> Sulphur

Test Data : [ 0.10572029  9.24506569 83.47119141 -0.6708293  -0.90309    -0.6189121
 -0.60206002 -0.6189121  -0.6708293  -0.6708293  -0.60206002] Predicted As ===> Sulphur

Test Data : [ 9.49363187e-02  1.03417597e+01  1.04952034e+02 -6.70829296e-01
 -9.03090000e-01 -6.18912101e-01 -6.02060020e-01 -6.70829296e-01
 -6.70829296e-01 -6.70829296e-01 -6.02060020e-01] Predicted As ===> Sulphur
```

In above reading test data and then using extension model predicting type of gas presents in leak where square brackets contains Test Data and after arrow symbol we can see predicted and identified Gas Leak Names

CONCLUSION

This study presents a novel approach using 3D-CNN and autoencoder-based techniques for gas detection in hyperspectral images, addressing environmental concerns arising from industrial activities. Leveraging spectral features and SAM distance calculation, the model accurately predicts gas emissions, contributing to pollution mitigation efforts. While the proposed 3D-CNN model achieves an 88% accuracy rate, an ensemble extension model, combining CNN, bidirectional, and GRU algorithms, achieves a higher accuracy of 93%. Through extensive experimentation and analysis, this study demonstrates the efficacy of the proposed methodology in accurately detecting gas leaks, paving the way for future advancements in environmental monitoring and pollution control.

REFERENCES:

[1] R. O. Green et al., “Imaging spectroscopy and the airborne visible/infrared imaging spectrometer (AVIRIS),” Remote Sens. Environ., vol. 65, no. 3, pp. 227–248, 1998.

[2] M. Govender, K. Chetty, and H. Bulcock, “A review of hyperspectral remote sensing and its application in vegetation and water resource studies,” Water Sa, vol. 33, no. 2, pp. 145–151, 2007.

[3] P. Y. Foucher and S. Doz, “Real time gas quantification using thermal hyperspectral imaging: Ground and airborne applications,” Accessed: Jan. 18, 2023. [Online]. Available: https://www.sto.nato.int/publications/ STO%20Meeting%20Proceedings/STO-MPSET-277/MP-SET-277- 18.pdf

[4] A. Vallières et al., “Algorithms for chemical detection, identification and quantification for thermal hyperspectral imagers,” in Proc. Chem. Biol. Standoff Detection III, vol. 5995, 2005, Art. no. 59950G.

[5] J.-M. Thériault, G. Fortin, F. Bouffard, H. Lavoie, P. Lacasse, and J. Lévesque, “Hyperspectral gas and polarization sensing in the LWIR: Recent results with MoDDIFS,” in Proc. 5th Workshop Hyperspectral Image Signal Process.: Evol. Remote Sens., 2013, pp. 1–4.

[6] D. W. Messinger, “Gaseous plume detection in hyperspectral images: A comparison of methods,” in Proc. Algorithms Technol. for Multispectral, Hyperspectral, Ultraspectral Imagery X, vol. 5425, 2004, pp. 592–603.

[7] M. Kastek, T. Piatkowski, R. Dulski, M. Chamberland, P. Lagueux, and V. Farley, “Method of gas detection applied to infrared hyperspectral sensor,” Photon. Lett. Poland, vol. 4, no. 4, pp. 146–148, 2012.

[8] F. Omruuzun and Y. Y. Cetin, “Endmember signature based detection of flammable gases in LWIR hyperspectral images,” in Proc. Adv. Environ., Chem., Biol. Sens. Technol. XII, vol. 9486, 2015, pp. 168–176.

[9] C. C. Funk, J. Theiler, D. A. Roberts, and C. C. Borel, “Clustering to improve matched filter detection of weak gas plumes in hyperspectral thermal imagery,” IEEE Trans. Geosci. Remote Sens., vol. 39, no. 7, pp. 1410–1420, Jul. 2001.

[10] D. R. Pogorzala, D. W. Messinger, C. Salvaggio, and J. R. Schott, "Gas plume species identification by regression analyses," in Proc. Algorithms Technol. for Multispectral, Hyperspectral, Ultraspectral Imagery X, vol. 5425, 2004, pp. 583–591.

[11] F. C. Robey, D. R. Fuhrmann, E. J. Kelly, and R. Nitzberg, "A CFAR adaptive matched filter detector," IEEE Trans. Aerosp. Electron. Syst., vol. 28, no. 1, pp. 208–216, Jan. 1992.

[12] T. S. Spisz, P. K. Murphy, C. C. Carter, A. K. Carr, A. Vallières, and M. Chamberland, "Field test results of standoff chemical detection using the FIRST," in Proc. Chem. Biol. Sens. VIII, vol. 6554, 2007.

[13] L. Sagiv, S. R. Rotman, and D. G. Blumberg, "Detection and identification of effluent gases by long wave infrared (LWIR) hyperspectral images," in Proc. IEEE 25th Conv. Elect. Electron. Engineers Isr., 2008, pp. 413–417.

[14] E. Hirsch and E. Agassi, "Detection of gaseous plumes in IR hyperspectral images using hierarchical clustering," Appl. Opt., vol. 46, no. 25, pp. 6368–6374, 2007.

[15] M. Kastek, T. Piatkowski, and P. Trzaskawka, "Infrared imaging fourier transform spectrometer as the stand-off gas detection system," Metrol. Meas. Syst., vol. 18, no. 4, pp. 607–620, 2011.

[16] P. Kuflik and S. R. Rotman, "Band selection for gas detection in hyperspectral images," in Proc. IEEE 27th Conv. Elect. Electron. Engineers Isr., 2012, pp. 1–4.

[17] S. Sabbah, R. Harig, P. Rusch, J. Eichmann, A. Keens, and J.-H. Gerhard, "Remote sensing of gases by hyperspectral imaging: System performance and measurements," Opt. Eng., vol. 51, no. 11, 2012, Art. no. 111717.

[18] ¸S. Öztürk, Y. Artan, and Y. E. Esin, "Ethene and CO2 gas detection in hyperspectral imagery," in Proc. 24th Signal Process. Commun. Application Conf. (SIU), 2016, pp. 357–360.

[19] J. Theiler and S. P. Love, "Algorithm development with on-board and ground-based components for hyperspectral gas detection from small satellites," in Proc. Algorithms, Technol., Appl. for Multispectral Hyperspectral Imagery XXV, vol. 10986, 2019.

[20] Y. C. Kim, H.-G. Yu, J.-H. Lee, D.-J. Park, and H.-W. Nam, "Hazardous gas detection for FTIR-based hyperspectral imaging system using DNN and CNN," in Proc. Electro-Opt. Infrared Syst.: Technol. Appl. XIV, vol. 10433, 2017.